

Curtius Reaction of Acetyl- and Fluorocarbonyl Azides

5.1 INTRODUCTION

Curtius rearrangement[Curtius, 1890] is the production of $N_2 + RNCO$ (isocyanate) from carbonyl azides $RC(O)N_3$ upon thermal or photochemical excitation. This reaction is useful in many areas of synthetic chemistry including medicinal chemistry[Ghosh *et al.*, 2018a,b; L'abbé, 1969]. Several experimental and theoretical studies investigating the mechanism of the Curtius reaction have been reported in the literature[Liu *et al.*, 2019; Xie *et al.*, 2018; Peng *et al.*, 2017; Feng *et al.*, 2017; Wu *et al.*, 2015; Deng *et al.*, 2016; Wan *et al.*, 2017b; Li *et al.*, 2017; Liu *et al.*, 2004; Ramos *et al.*, 2012; Kubicki *et al.*, 2011; Tarwade *et al.*, 2008; Wu *et al.*, 2017; Li *et al.*, 2015; Kakkar *et al.*, 2009; Banert *et al.*, 2012; Wan *et al.*, 2017a; Zabalov and Tiger, 2005; Pritchina *et al.*, 2003; Wilde *et al.*, 1971; Zeng *et al.*, 2013; Sun *et al.*, 2015; Linke *et al.*, 1967; Tisue *et al.*, 1967; Lwowski and Tisue, 1965; Sigman *et al.*, 1988; Autrey and Schuster, 1987; Kubicki *et al.*, 2009; Yukawa and Tsuno, 1957; Abu-Eittah *et al.*, 2006; Faustov *et al.*, 2003]. Two mechanisms viz., a stepwise and a concerted pathway have been proposed. The stepwise mechanism involves the formation of a nitrene $RC(O)N$ by N_2 elimination, followed by an intramolecular rearrangement of the nitrene yielding the isocyanate. In the concerted mechanism, elimination of N_2 and $N-C$ bond formation to form the isocyanate occur simultaneously. Previous mechanistic studies of Curtius reaction have indicated that thermal reactions usually follow concerted mechanism[Zabalov and Tiger, 2005; Linke *et al.*, 1967; Liu *et al.*, 2004; Ramos *et al.*, 2012; Tarwade *et al.*, 2008] with retention of configuration and photochemical reactions follow both concerted and stepwise mechanisms[Tisue *et al.*, 1967; Wu *et al.*, 2017; Liu *et al.*, 2019; Peng *et al.*, 2017; Lwowski and Tisue, 1965]. For example, electronic structure calculations have provided strong support for concerted mechanism under thermal conditions for chlorodifluoroacetyl azide,[Ramos *et al.*, 2012] formyl azide,[Kakkar *et al.*, 2009; Banert *et al.*, 2012] cyclopropyl and cyclopropenoyl azides[Tarwade *et al.*, 2008]. Photochemical studies of 4-acetylbenzoyl azide,[Sigman *et al.*, 1988] β -naphthoyl azide and carbethoxy azide,[Autrey and Schuster, 1987] benzoyl and pivavoyl azide,[Kubicki *et al.*, 2009] nicotinoyl and isonicotinoyl azide,[Liu *et al.*, 2019] difluoroacetyl azide[Feng *et al.*, 2017] have shown the formation of nitrenes and point to a stepwise mechanism.

The reactant carbonyl azide exists in syn and anti conformers and the transformation between the structures happens[Liu *et al.*, 2004; Sun *et al.*, 2015] via out-of-plane rotation of the N_3 group. Electronic structure calculations[Liu *et al.*, 2004] have shown that syn is more stable than the corresponding anti conformer by a few kcal/mol energy. Concerted pathway involves the syn while the stepwise mechanism originates from the higher energy anti isomer. Reaction energies and barrier heights for the Curtius reaction depend upon[Liu *et al.*, 2004] the substituent R group in the azide $RC(O)N_3$. Yukawa *et al.*[Yukawa and Tsuno, 1957] found that rate of the Curtius reaction changed depending upon whether electron withdrawing or electron donating groups were present at the *m*-position of benzazide. In the present work, the Curtius rearrangement reaction of acetyl azide ($CH_3C(O)N_3$) and fluorocarbonyl azide ($FC(O)N_3$) under thermal conditions were investigated. The CH_3 and F substituents are isoelectronic but have opposing effects in the local electronic environment. Further, the two substituents do not impose any steric effects and are almost similar in size.

Abu-Eittah *et al.* has predicted stepwise decomposition for $\text{CH}_3\text{C}(\text{O})\text{N}_3$ based on MP2 level electronic structure theory calculations [Abu-Eittah *et al.*, 2006]. On the other hand, concerted pathway was found to have lower energy barrier than that of stepwise pathway at the CBS-QB3 level of theory [Liu *et al.*, 2004] and B3LYP/6-311+G(d,p) and CCSD(T)/6-311+G(d,p) theories [Tarwade *et al.*, 2008]. The nitrene $\text{CH}_3\text{C}(\text{O})\text{N}$ has not been experimentally identified as a Curtius reaction intermediate. Production of nitrenes under thermal conditions in the gas phase is usually not considered to be effective. The triplet nitrene $\text{FC}(\text{O})\text{N}$ produced by the decomposition of matrix-isolated $\text{FC}(\text{O})\text{N}_3$ by ArF excimer laser photolysis has been detected [Zeng *et al.*, 2011]. Jenks and co-workers [Sun *et al.*, 2015] have successfully characterized $\text{FC}(\text{O})\text{N}$ in the gas phase under thermal conditions. Using the flash pyrolysis technique, 49% yield of the triplet $\text{FC}(\text{O})\text{N}$ was recorded in these experiments. CBS-QB3 and B3LYP/6-311+G(3df) calculations [Sun *et al.*, 2015] for the decomposition of $\text{FC}(\text{O})\text{N}_3$ have shown that the nitrene formation transition state (TS) lies at a lower energy in comparison to the concerted TS. In a similar system, $\text{CH}_3\text{OC}(\text{O})\text{N}_3$, in which the substituent CH_3O group has a similar electronic effect as F, stepwise pathway was found to have lower barrier than the concerted pathway. However, attempts to detect the methoxycarbonyl nitrene $\text{CH}_3\text{OC}(\text{O})\text{N}$ via decomposition of $\text{CH}_3\text{OC}(\text{O})\text{N}_3$ were unsuccessful [Liu *et al.*, 2004; Wilde *et al.*, 1971; Dyke *et al.*, 2005]. In another study, [Wu *et al.*, 2015] structurally similar difluorophosphoryl nitrene $\text{F}_2\text{P}(\text{O})\text{N}$ was observed in the gas phase by the flash vacuum pyrolysis of difluorophosphoryl azide. Xie *et al.* [Xie *et al.*, 2018] have studied the photo-induced Curtius reaction of $\text{FC}(\text{O})\text{N}_3$ using QM/MM nonadiabatic dynamics simulations. The azide molecule jumped into S_3 state upon irradiation by 193 nm light. After a series of non-radiative transitions, the system evolved into the S_0 state and the Curtius rearrangement occurred over a period of 300 fs following the stepwise mechanism. The rearrangement reaction $\text{FC}(\text{O})\text{N} \longrightarrow \text{FNCO}$ was observed only in the S_0 state.

In the work presented here, Curtius reaction of $\text{CH}_3\text{C}(\text{O})\text{N}_3$ and $\text{FC}(\text{O})\text{N}_3$ were studied in the gas phase under thermal conditions. The investigation was carried out using electronic structure theory calculations and Born-Oppenheimer direct dynamics simulations [Sun and Hase, 2003; Paranjothy *et al.*, 2013]. The primary objective is to study the effect of substituent on the Curtius rearrangement under similar reaction conditions. Classical trajectories with similar initial conditions for both the molecules were launched and the ensuing reaction dynamics investigated.

5.2 POTENTIAL ENERGY SURFACE

Stationary points on the potential energy surface of $\text{CH}_3\text{C}(\text{O})\text{N}_3$ and $\text{FC}(\text{O})\text{N}_3$ were characterized with different electronic structure theory methods using 6-31+G* basis set. These methods were selected based on previous electronic structure theory studies [Sherman and Jenks, 2014; Sun *et al.*, 2015; Liu *et al.*, 2004; Abu-Eittah *et al.*, 2006] on these two systems. Equilibrium points and transition states (TSs) were geometry optimized and normal mode frequency calculations were performed to differentiate an equilibrium point from a TS. Further, intrinsic reaction coordinate (IRC) calculations were performed to make sure a given TS connects correct reactant with correct products. The results of these calculations are summarized in Table 5.1 wherein the classical energies (zero point energy not corrected) are given in kcal/mol units. The energies given are relative to the respective syn conformer. The benchmark CCSD(T) single point calculations were performed using MP2 optimized geometries. Among the various methods shown in Table 5.1, B3LYP/6-31+G* was selected to perform the direct dynamics simulations considering the accuracy and the computational cost associated with this method. Mean absolute deviation (MAD) from the benchmark CCSD(T) calculations of the B3LYP, PBE0, and M06-2X methods is 4.6 (5.0), 8.8 (10.1), and 6.0 (7.7) kcal/mol, respectively, for the $\text{CH}_3\text{C}(\text{O})\text{N}_3$ ($\text{FC}(\text{O})\text{N}_3$) system. Clearly, the B3LYP functional shows the least MAD from the benchmark CCSD(T) calculation among the density functionals considered in the present work. Figure 5.1

shows the potential energy profiles of $\text{CH}_3\text{C}(\text{O})\text{N}_3$ and $\text{FC}(\text{O})\text{N}_3$ dissociation computed using the B3LYP/6-31+G* method. Optimized geometries of the stationary points are given in Figures 5.2 and 5.3.

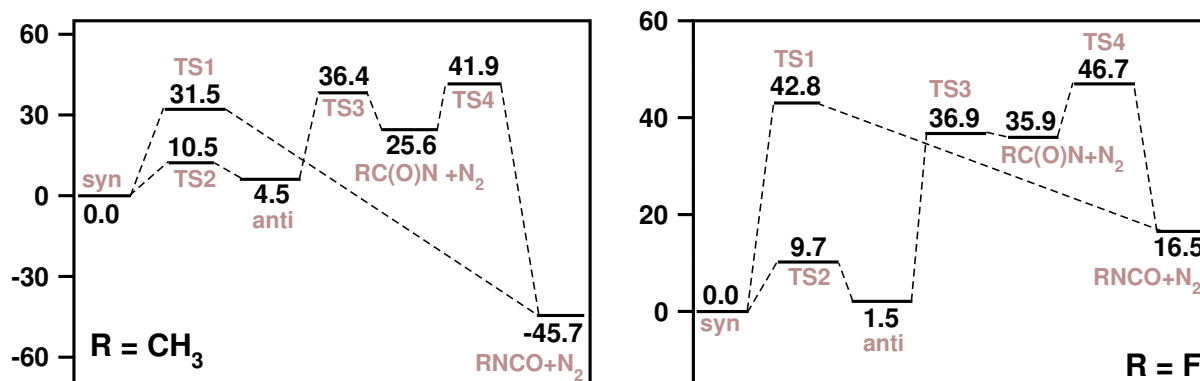


Figure 5.1 : Dissociation energy profiles of $\text{RC}(\text{O})\text{N}_3$ ($\text{R} = \text{CH}_3$ and F) computed using B3LYP/6-31+G* level of electronic structure theory. Energies are given in kcal/mol units and zero point energy not corrected.

Table 5.1 : Comparison of stationary point energies (in kcal/mol) on the dissociation energy profiles of $\text{RC}(\text{O})\text{N}_3$ ($\text{R} = \text{CH}_3$ and F) computed using different methods with 6-31+G* basis set. Energies given are relative to the respective syn conformer without zero-point energy corrections.

stationary point	B3LYP ^a	PBE0	M06-2X	MP2	CCSD(T) ^b
syn- $\text{CH}_3\text{C}(\text{O})\text{N}_3$	0.0	0.0	0.0	0.0	0.0
TS1 ^c	31.5	36.9	33.1	38.6	27.0
$\text{CH}_3\text{NCO} + \text{N}_2$	-45.7	-39.7	-47.1	-49.5	-51.6
TS2 ^d	10.5	10.7	11.8	10.6	10.5
anti- $\text{CH}_3\text{C}(\text{O})\text{N}_3$	4.5	4.4	4.9	4.5	5.2
TS3 ^e	36.4	42.7	41.4	45.9	31.2
$\text{CH}_3\text{C}(\text{O})\text{N}$	25.6	32.3	27.0	22.1	13.9
TS4 ^f	41.9	50.8	45.5	53.6	33.2
syn- $\text{FC}(\text{O})\text{N}_3$	0.0	0.0	0.0	0.0	0.0
TS1 ^c	42.8	51.0	47.2	48.5	36.2
$\text{FNCO} + \text{N}_2$	16.5	24.2	18.3	15.2	9.1
TS2 ^d	9.7	10.1	11.1	10.1	9.7
anti- $\text{FC}(\text{O})\text{N}_3$	1.5	1.8	2.2	1.7	1.9
TS3 ^e	36.9	44.4	42.1	45.7	30.3
$\text{FC}(\text{O})\text{N}$	35.9	43.7	39.8	35.0	25.2
TS4 ^f	46.7	56.4	52.1	56.7	38.6

^a method used in the dynamics simulations

^b CCSD(T) single point energies were computed using MP2 optimized geometries

^c concerted TS connecting syn conformer with $\text{RNCO} + \text{N}_2$

^d connects syn conformer with anti

^e connects anti conformer with $\text{RC}(\text{O})\text{N} + \text{N}_2$

^f connects $\text{RC}(\text{O})\text{N}$ with RNCO

Decomposition of $\text{CH}_3\text{C}(\text{O})\text{N}_3$ is highly exoergic with the $\text{CH}_3\text{NCO} + \text{N}_2$ products having energy of -45.7 kcal/mol relative to syn conformer. For this molecule, concerted transition state

(TS1) is lower in energy than the nitrene formation TS by 4.9 kcal/mol. This trend is similar to ΔG (298 K) values computed at the B3LYP/6-311+G**//B3LYP/6-31G* and CBS-QB3 theories by Liu *et al.*[Liu *et al.*, 2004] IRC calculations showed that TS1 is connected to the syn conformer and TS3 is connected to the high energy anti conformer of the reactant. For $\text{FC}(\text{O})\text{N}_3$, the reaction is endoergic by 16.5 kcal/mol. For this system, concerted TS has 5.9 kcal/mol higher energy than the nitrene formation TS, indicating the preference for stepwise mechanism. CBS-QB3 and B3LYP/6-311+G(3df) calculations showed that concerted TS has 6.9 and 5.7 kcal/mol energy higher than the respective nitrene formation TSs[Sun *et al.*, 2015]. Electronic structure theory data shown in Table 5.1 are in agreement with these predictions. Note that the overall reaction barrier is higher for the stepwise pathway for both the molecules (see TS4 energies for both the molecules). Nevertheless, the differences in the barrier heights for the concerted and stepwise paths are not more than 10 kcal/mol at any level of theory.

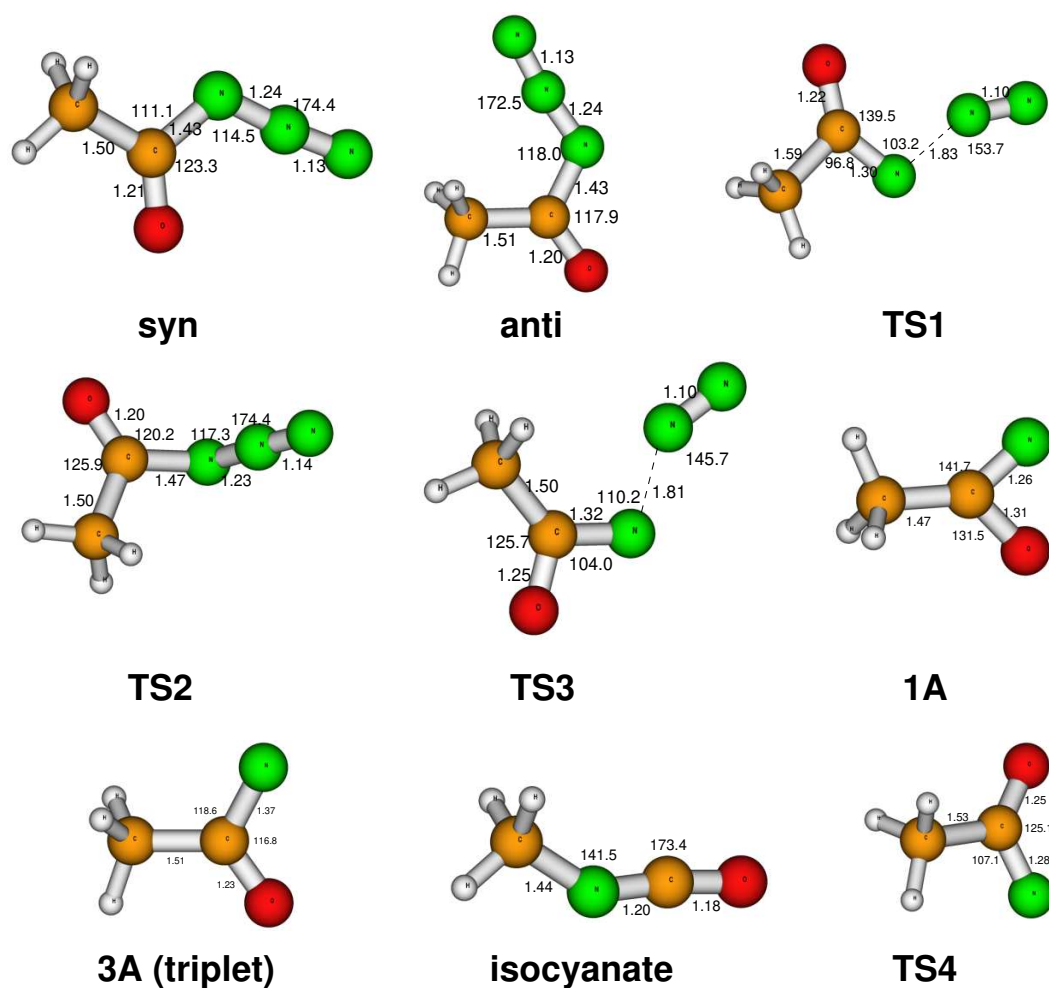


Figure 5.2 : Optimized geometries of the stationary points on the $\text{CH}_3\text{C}(\text{O})\text{N}_3$ potential energy surface

To study the atomic level mechanisms of the Curtius reaction of $\text{CH}_3\text{C}(\text{O})\text{N}_3$ and $\text{FC}(\text{O})\text{N}_3$, Born-Oppenheimer direct dynamics simulations[Sun and Hase, 2003; Paranjothy *et al.*, 2013] at the B3LYP/6-31+G* level of electronic structure theory was performed. Classical trajectories were launched from the low energy syn conformer with fixed total energies. For each molecule, simulations were performed at two different total energies $E_{\text{tot}} = 90$ and 120 kcal/mol. These values were selected because both the reaction pathways will be accessible at these energies and the

simulations can be completed in a reasonable amount of computational time. The energies were distributed among the normal mode vibrations of the molecule using classical micro-canonical sampling algorithm[Peslherbe *et al.*, 1999; Hase and Buckowski, 1980]. The trajectories were propagated till 4 ps or until the reaction products were separated by a distance of 15 Å. The integrations were performed using a 6th order Symplectic integrator[Schlier and Seiter, 1998, 2000] with a stepsize of 0.5 fs. The time evolved positions and momenta were recorded every 5 fs during the trajectory integrations. These conditions were sufficient to maintain energy conservation within $E_{\text{tot}} \pm 1.0$ kcal/mol.

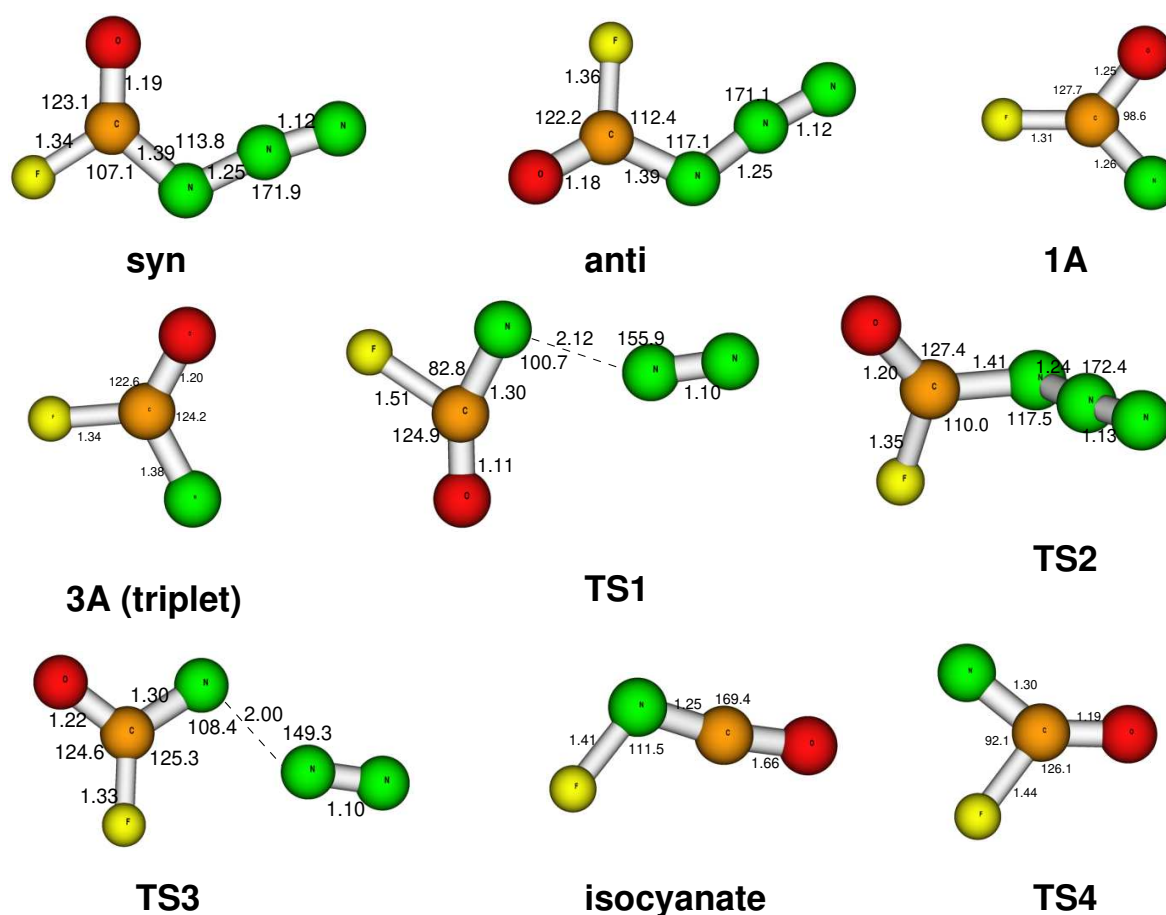


Figure 5.3 : Optimized geometries of the stationary points on the FC(O)N_3 potential energy surface

5.3 RESULTS AND DISCUSSION

In each simulation, 200 trajectories were generated which accounts to a total of 800 trajectories (two simulations with different E_{tot} per molecule). Trajectories were analyzed for reaction mechanisms, branching ratios, lifetimes, etc. In all the trajectories, total energy was conserved within $E_{\text{tot}} \pm 1.0$ kcal/mol. Total energy as a function of time for a few trajectories are given in Figure 5.4.

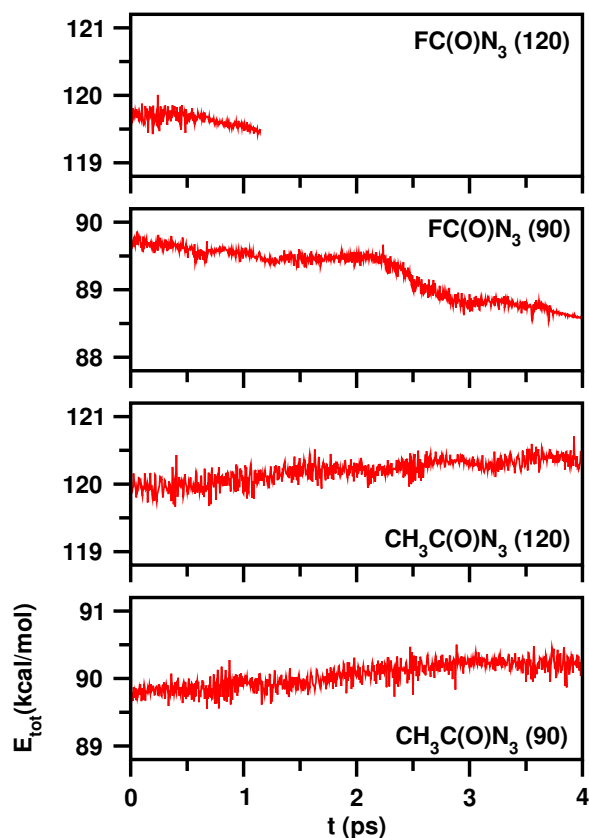


Figure 5.4 : Total energy as a function of time for a few sample classical trajectories. In all plots, x-axes ranges are same, y-axes show total energy in units of kcal/mol.

Reactivity (number of trajectories showing dissociation within the stipulated integration time) was less for $\text{CH}_3\text{C}(\text{O})\text{N}_3$ in comparison to $\text{FC}(\text{O})\text{N}_3$. This is because the former has more vibrational degrees of freedom than the latter and the average available energy per vibrational degree of freedom is low. At $E_{\text{tot}} = 90$ kcal/mol, 9% and 90% reactivity was observed for $\text{R} = \text{CH}_3$ and F , respectively. In the high energy simulations ($E_{\text{tot}} = 120$ kcal/mol), reactivity increased to 57.5% ($\text{R} = \text{CH}_3$) and 100% ($\text{R} = \text{F}$).

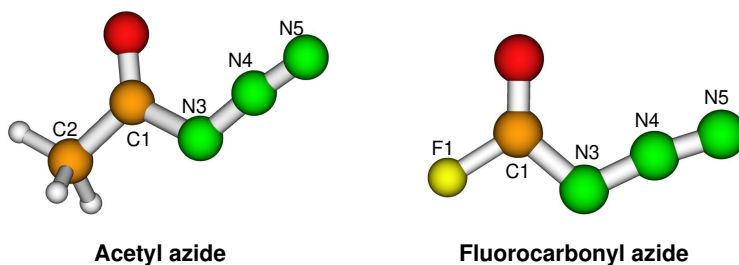


Figure 5.5 : Numbering system used for discussion purposes in the text.

5.3.1 Dynamics of $\text{CH}_3\text{C}(\text{O})\text{N}_3$

We observed dissociation of acetyl azide in 18 and 115 trajectories at $E_{\text{tot}} = 90$ and 120 kcal/mol, respectively. Using the numbering system shown in Figure 5.5, breaking of $\text{N}_3\text{-N}_4$

bond and formation of C2-N3 bond occur simultaneously in the concerted pathway. In the stepwise mechanism, N3-N4 bond dissociates first resulting in nitrene and after a finite lifetime, rearrangement of the nitrene to the isocyanate occurs. Time evolved N3-N4 and C2-N3 bond distances (in Å units) extracted from all the reactive trajectories of $\text{CH}_3\text{C}(\text{O})\text{N}_3$ are given in Figure 5.6 and data from three sample trajectories are shown in Figure 5.7(a).

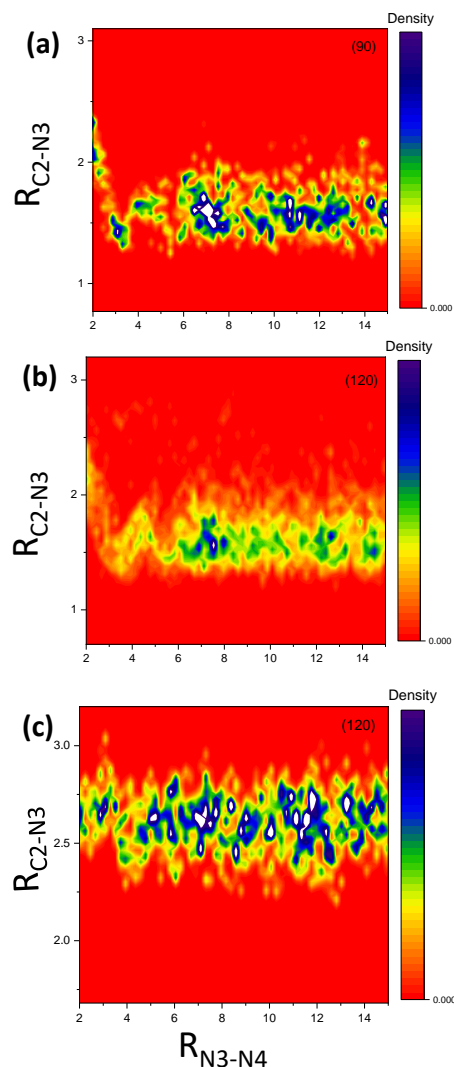


Figure 5.6 : Density plots (a), (b), and (c) show time evolved N3-N4 (x -axes) and C2-N3 (y -axes) bond distances (in Å) for $\text{CH}_3\text{C}(\text{O})\text{N}_3$ dissociation. (a) shows data from $E_{\text{tot}} = 90$ kcal/mol simulation, (b) and (c) show data from 120 kcal/mol simulation. Red, and Blue colors correspond to minimum and maximum density respectively.

Time evolved bond distances data of $\text{CH}_3\text{C}(\text{O})\text{N}_3$ system are shown in the three density plots (see Figure 5.6). Here the color bar varies from red to blue with the increase in density (red color for the lowest density, and blue color is for the highest density). Trajectory data from $E_{\text{tot}} = 90$ kcal/mol simulation (see Figure 5.6) shows that all the reactive trajectories follow the concerted pathway. This is consistent with electronic structure calculations that the concerted TS has 4.9 kcal/mol lower energy than the nitrene formation TS. However, the difference is not so large that trajectories can be expected to sample the stepwise region of the potential energy surface in the high energy (120 kcal/mol) simulation. We observed a small number of trajectories forming the

nitrene intermediate $\text{CH}_3\text{C}(\text{O})\text{N}$. Out of the 115 reactive trajectories in the 120 kcal/mol simulation, nitrene formation occurred in 22 trajectories ($\approx 19\%$). Among these trajectories, only 4 showed intramolecular rearrangement of the nitrene to form the final product CH_3NCO within the total integration time of 4 ps. In the other 18 trajectories, nitrene intermediate existed till the calculations were stopped. We believe isocyanate formation ($\text{CH}_3\text{C}(\text{O})\text{N} \rightarrow \text{CH}_3\text{NCO}$) will occur if these trajectories were run for a longtime. Figure 5.6 shows bond distances extracted from trajectories resulting in the final isocyanate product (concerted = 93, stepwise = 4) from the 120 kcal/mol simulation and similar data from 18 trajectories forming only the nitrene. In Figure 5.7(a), bond distances from sample trajectories showing concerted pathway (red circles), stepwise pathway leading to the final product (blue triangle), and nitrene formation (green squares) via the stepwise pathway are presented.

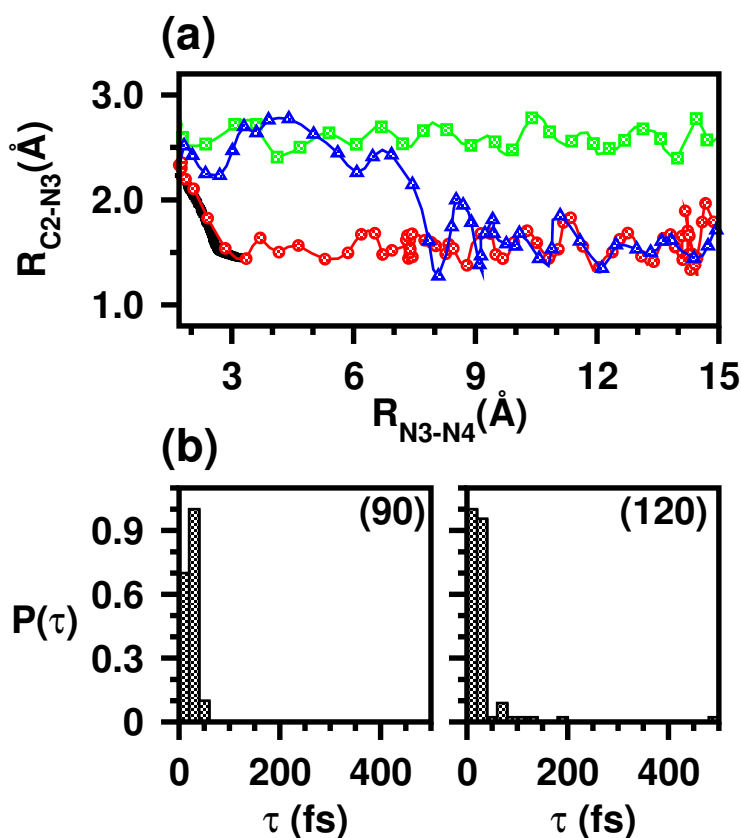


Figure 5.7 : (a) shows time evolved $\text{N}_3\text{-N}_4$ and $\text{C}_2\text{-N}_3$ bond distances (in Å) for $\text{CH}_3\text{C}(\text{O})\text{N}_3$ dissociation for a few sample trajectories. Red circles correspond to a concerted trajectory and blue triangles correspond to a stepwise trajectory resulting in the CH_3NCO final product. The green squares correspond to a stepwise trajectory existing as nitrene when the calculation was stopped. The black thick line in this plot is the IRC data for the concerted pathway. (b) shows lifetimes τ (in fs) of the intermediate nitrene species calculated from the trajectories.

From all the reactive trajectories forming the final products $\text{CH}_3\text{NCO} + \text{N}_2$, the lifetime τ associated with the $\text{CH}_3\text{C}(\text{O})\text{N}$ intermediate was computed as follows. If t_1 is the time at which the dissociating $\text{N}_3\text{-N}_4$ bond reaches 2.1 Å and t_2 is the time at which $\text{C}_2\text{-N}_3$ distance decreases to 1.4 Å, then $\tau = t_2 - t_1$. These critical values are selected based on the equilibrium geometry parameters of relevant stationary points on the potential energy surface which are presented in Figures 5.2 and 5.3. Figure 5.7(b) shows distributions of τ from 90 and 120 kcal/mol simulations.

Note that only data from 5.6(b) is used in calculating τ for the 120 kcal/mol simulation i.e., only those trajectories that resulted in the final products were considered. All the trajectories in the low energy simulation reacted via concerted pathway and consistently τ is less than 60 fs. In the high energy simulation, a few trajectories formed the final product via the stepwise pathway and is reflected in the $P(\tau)$ distribution i.e., relatively larger τ values. Overall, concerted mechanism is preferred for the Curtius reaction of acetyl azide under the current simulation conditions. This preference is driven by the large exoergicity of the reaction (-45.7 kcal/mol) and relatively smaller barrier for the concerted pathway (31.5 kcal/mol) in comparison to the nitrene formation barrier (36.4 kcal/mol). Snapshots of example $\text{CH}_3\text{C}(\text{O})\text{N}_3$ trajectories dissociating via concerted and stepwise pathways are shown in Figures 5.8(a) and (b), respectively. The numbers inside every frame is the time (in fs) at which the snapshot was taken. For the concerted trajectory, N3-N4 dissociation and C2-N3 bond formation can be seen in the 940 fs frame. In the stepwise trajectory, N3-N4 dissociation occurs around 3080 fs. The nitrene has a lifetime of roughly 200 fs and the intramolecular rearrangement $\text{CH}_3\text{C}(\text{O})\text{N} \rightarrow \text{CH}_3\text{NCO}$ can be observed in the 3300 fs frame.

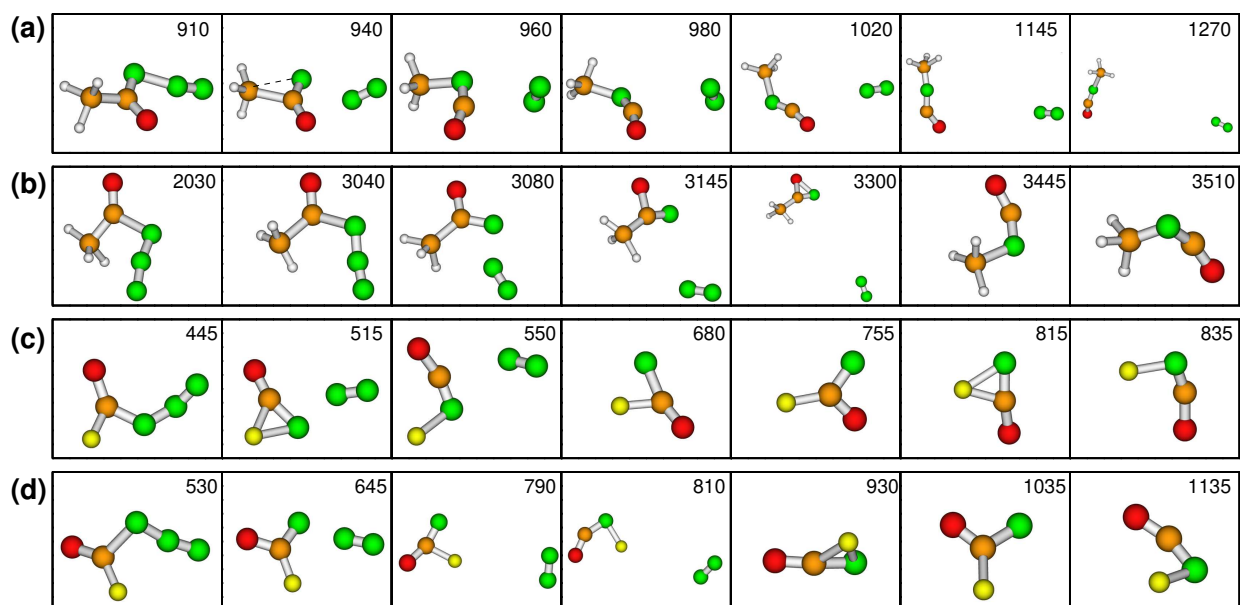


Figure 5.8 : Snapshots of few example trajectories, (a) concerted $\text{CH}_3\text{C}(\text{O})\text{N}_3$ dissociation; (b) stepwise $\text{CH}_3\text{C}(\text{O})\text{N}_3$ dissociation; (c) concerted $\text{FC}(\text{O})\text{N}_3$ dissociation followed by $\text{FNCO} \leftrightarrow \text{FC}(\text{O})\text{N}$ isomerization; (d) $\text{FC}(\text{O})\text{N}_3$ stepwise dissociation followed by $\text{FNCO} \rightarrow \text{FC}(\text{O})\text{N}$ isomerization. The numbers inside each frame is time in fs at which the snapshot was taken.

5.3.2 Dynamics of $\text{FC}(\text{O})\text{N}_3$

As mentioned earlier, enhanced reactivity was observed for the dissociation of $\text{FC}(\text{O})\text{N}_3$. At $E_{\text{tot}} = 90$ and 120 kcal/mol, 180 and 200 trajectories underwent dissociation, respectively. Triplet $\text{FC}(\text{O})\text{N}$ has been detected in experiments[Zeng *et al.*, 2011; Sun *et al.*, 2015] during the decomposition of $\text{FC}(\text{O})\text{N}_3$ indicating the operation of stepwise mechanism. Hence, an increased number of trajectories are expected to show stepwise mechanism in the simulations which is indeed the case. In Figure 5.9, bond distance data from all the reactive trajectories are shown. Time evolved bond distances for three select trajectories and lifetimes of the intermediate nitrene species computed from the trajectories are presented in Figure 5.10.

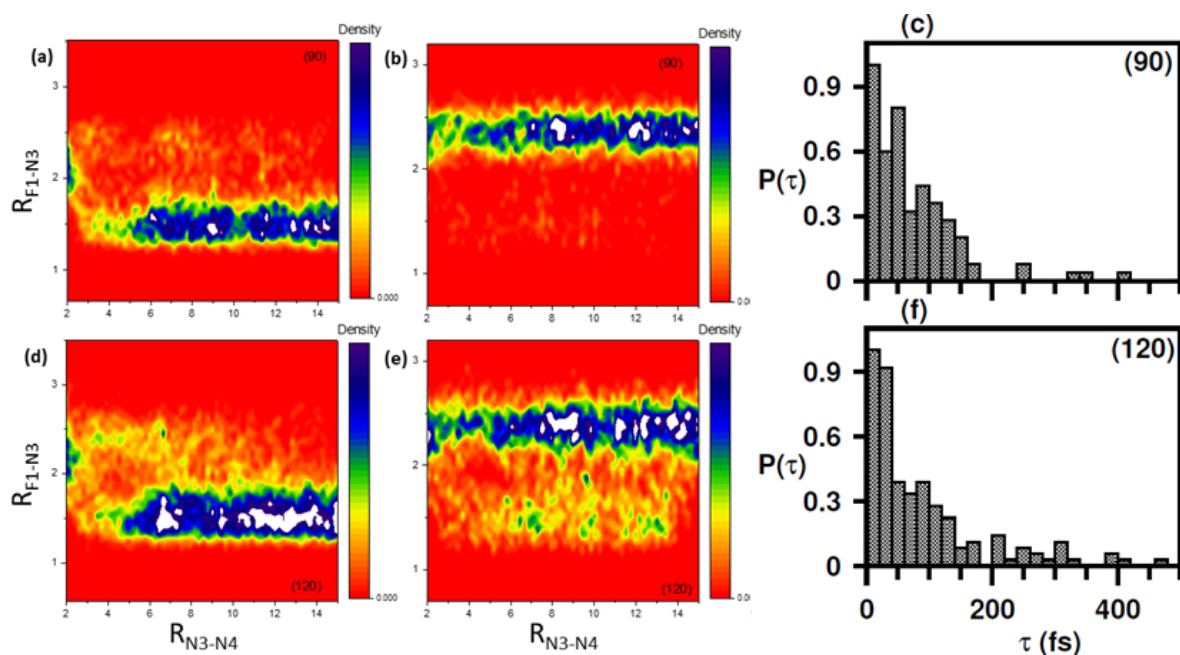


Figure 5.9 : Time evolved N3-N4 and F1-N3 bond distances (in Å) computed from the FC(O)N₃ trajectories are shown in density plots (a), (b), (d), and (e). Distributions of lifetimes τ (in fs) of the intermediate nitrene species are shown in (c) and (f). Top panels show data from the low energy ($E_{\text{tot}} = 90$ kcal/mol) simulation and the bottom panels show results of high energy (120 kcal/mol) simulation. Red, and Blue colors correspond to minimum and maximum density respectively.

Lifetime of FC(O)N was calculated in a similar way as that for CH₃C(O)N using the optimized geometry parameters. The time at which N3-N4 distance reaches 2.3 Å was taken as t_1 and the time at which F1-N3 distance decreases to 1.4 Å was taken as t_2 and $\tau = t_2 - t_1$. In comparison to acetyl azide dynamics, an enhanced number of trajectories follow stepwise mechanism. At $E_{\text{tot}} = 90$ kcal/mol, 107 trajectories resulted in the FNCO + N₂ products, out of which 26 followed the stepwise mechanism. This fraction is approximately 24%. Note that this does not include another 73 trajectories forming only the nitrene intermediate when the calculation was stopped (shown in Figure 5.9(b)). An interesting aspect observed in Figure 5.9(b) is that 4 out of 73 nitrene formation trajectories followed the concerted mechanism. These trajectories resulted in the final products FNCO + N₂ via the concerted mechanism but the isocyanate isomerized to the nitrene FC(O)N. The barrier for this isomerization (FNCO \rightarrow FC(O)N) is 30.2 kcal/mol (see Figure 5.1). Considering the stepwise trajectories forming the final product and also the nitrene, overall fraction of trajectories following the stepwise mechanism enhances to $\approx 52\%$. In the 120 kcal/mol simulation, all the 200 trajectories were reactive. A total of 141 trajectories formed the final reaction products at $E_{\text{tot}} = 120$ kcal/mol. Among them, 87 trajectories followed concerted and 54 dissociated via the stepwise mechanism. 59 trajectories formed the nitrene product and 18 of these dissociated via the concerted mechanism followed by isomerization of FNCO to the nitrene form. Combining together the stepwise trajectories forming the final product and ending up as nitrene, a fraction of 48% is obtained in the 120 kcal/mol simulation for the stepwise trajectories. The fraction of stepwise trajectories obtained in the simulations of fluorocarbonyl azide is larger than that for acetyl azide. These fractions are in agreement with experimental predictions.[Zeng *et al.*, 2011; Sun *et al.*, 2015] Note that Sun *et al.*[Sun *et al.*, 2015] had estimated 49% yield for the formation of FC(O)N in their pyrolysis experiments.

An important observation from the bond distance plots shown in Figure 5.9 is that concerted mechanism was followed in some trajectories but the resulting isocyanate isomerized to the nitrene form. This was also seen in the stepwise trajectories. The $\text{FNCO} \longleftrightarrow \text{FC(O)N}$ isomerization (both forward and reverse) played an important role in determining the trajectory fractions. This indicates that the nitrene species detected in the experiments might also be resulting via the concerted mechanism followed by isomerization provided sufficient amount of energy was available. This is an indirect pathway resulting in the nitrene and may be occurring in the experiments to some extent. Note that this behavior was not observed in the simulation of $\text{CH}_3\text{C(O)N}_3$. For this system, the overall reaction is highly exoergic (-45.7 kcal/mol, see Figure 5.1) and the isomerization of CH_3NCO to $\text{CH}_3\text{C(O)N}$ has a barrier of 87.6 kcal/mol.

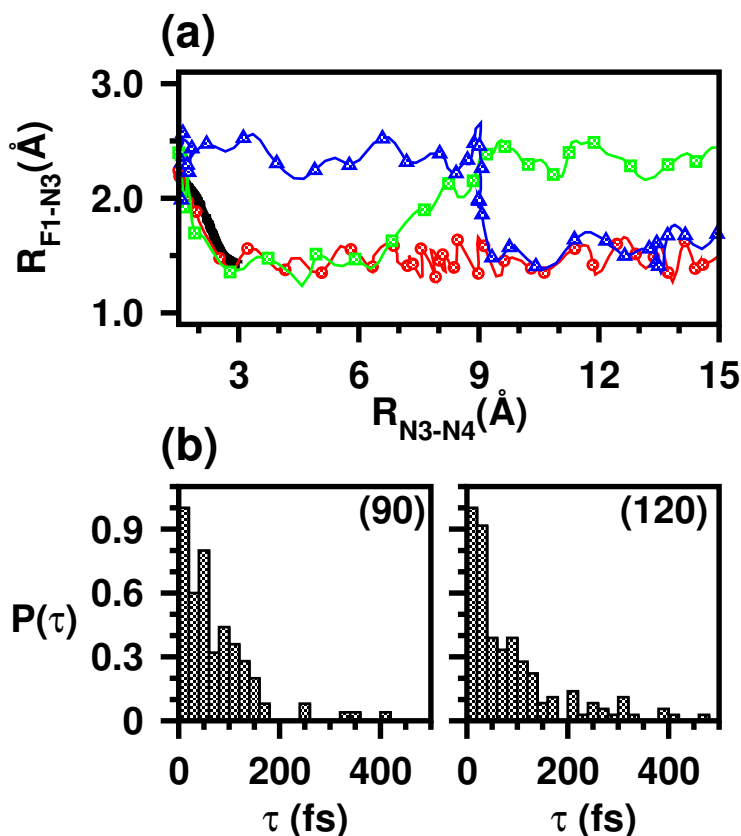


Figure 5.10 : Time evolved $\text{N}_3\text{-N}_4$ and F1-N_3 bond distances (in Å) of the FC(O)N_3 system, for a concerted trajectory (red circles), stepwise trajectory (blue triangles), and a concerted trajectory forming the nitrene intermediate (green squares). The black thick line in this plot is the IRC data for the concerted pathway. Distributions of lifetimes τ (in fs) of the intermediate nitrene species are shown in (b).

Figure 5.10(a) shows example trajectories dissociating via concerted pathway (red circles), stepwise pathway (blue triangles), and an indirect trajectory (green squares) forming FNCO via the concerted pathway but isomerizing back to the nitrene (FC(O)N). These plots clearly demonstrate the operation of various dissociation mechanisms of FC(O)N_3 . Distributions of lifetimes $P(\tau)$ shown in 5.10(b) are different from those of acetyl azide discussed above. For FC(O)N , the distributions extend till 800 fs. For comparison with $\text{CH}_3\text{C(O)N}$, the plots are shown till 500 fs only. On the average, fluorocarbonyl nitrene has a longer lifetime in comparison to acetyl nitrene. In computing the lifetimes, those trajectories ending up as nitrene were not included.

Inspection of the nitrene formation trajectories showed that the lifetimes of these intermediates are much longer indicating enhanced stability of FC(O)N in the gas phase. Snapshots of example trajectories showing concerted and stepwise dissociation of FC(O)N₃ are given in Figures 5.8(c) and (d), respectively. In the concerted trajectory, dissociation of N3-N4 and the formation of F1-N3 bond can be seen in the 515 fs frame. Further, isomerization of FNCO to the nitrene form and the corresponding reverse isomerization can be observed in the 680 and 815 fs frames, respectively. This trajectory shows the formation of nitrene via the concerted mechanism. Figure 5.8(d) shows stepwise reaction of FC(O)N₃. N3-N4 dissociation resulting in FC(O)N + N₂ (645 fs), FC(O)N → FNCO isomerization (810 fs), FNCO → FC(O)N isomerization (930 fs) and the reverse isomerization (1135 fs) can be observed.

Sun et al.[Sun *et al.*, 2015] have proposed the following mechanism for the observation of FNCO in their pyrolysis experiments. Following the stepwise mechanism, singlet FNCO is formed which undergoes intersystem crossing (ISC) to form the triplet FNCO which is stable by 7.9 kcal/mol (CBS-QB3) in comparison to the singlet. However, the triplet species must undergo reverse ISC to form the final isocyanate product. This is because CBS-QB3 calculations showed no lower energy pathway to form the final product from the triplet nitrene. Note that FC(O)N → FNCO isomerization was observed only in the S₀ state in the QM/MM nonadiabatic dynamics simulations of FC(O)N₃ dissociation performed by Xie et al.[Xie *et al.*, 2018]. At the B3LYP/6-31+G* theory, the triplet FNCO is stable by 15.3 kcal/mol relative to the singlet. The simulations performed here show that even as singlet, average lifetime of fluorocarbonyl nitrene is larger than acetyl nitrene indicating that the Curtius reaction of FC(O)N₃ occurs by both concerted and stepwise mechanisms. In the pyrolysis experiments of FC(O)N₃, the FCO radical was also observed[Sun *et al.*, 2015]. Based on electronic structure calculations, it was rationalized that the FCO radical was not produced by direct homolytic dissociation of the parent azide species. The FCO radicals were probably formed by an indirect mechanism involving the dimerization of nitrene and subsequent dissociation. In the dynamics simulations, the homolytic dissociation of FC(O)N₃ was not observed even-though sufficient amount of energy was available, confirming the earlier prediction[Sun *et al.*, 2015].

5.4 SUMMARY

Chemical dynamics simulations were performed to study the atomic level mechanisms of Curtius reaction of acetyl azide and fluorocarbonyl azide under thermal conditions. Competition between two possible mechanisms, concerted *vs.* stepwise, was investigated for both the systems. The CH₃ and F substituents in these two molecules are isoelectronic, similar in size, and do not have any steric effects. Changing the substituent from the electron donating CH₃ group to the electron withdrawing F changes the potential energy landscape (see Figure 5.1). The dynamics simulations were performed using density functional B3LYP/6-31+G* level of theory at fixed total energies. The available energy was distributed among the normal mode vibrations of the molecules in the electronic ground state mimicking thermal reaction conditions. Enhanced reactivity for FC(O)N₃ in comparison to CH₃C(O)N₃ was observed at same E_{tot} due to differences in the average energy available per mode. We also ran 40 trajectories for the CH₃C(O)N₃ system with the same average energy available per mode as the 120 kcal/mol simulation for FC(O)N₃. All the 40 trajectories showed reaction within the stipulated integration time, a scenario similar to 120 kcal/mol simulation of FC(O)N₃. This clearly shows that the observed reactivity was related to the available energy in the trajectories and no other factors were influencing it.

For acetyl azide, major fraction of the trajectories showed concerted mechanism. Under similar simulation conditions, the nature of the dynamics changed when the substituent changed from CH₃ to F. Roughly 50% of trajectories showed stepwise mechanism with appreciable lifetimes

for the associated nitrene species. This is in agreement with an earlier thermal experiment[Sun *et al.*, 2015] on the Curtius reaction of FC(O)N_3 . The general consensus about the mechanism of Curtius reaction is that thermal reactions prefer concerted mechanism and photochemical reactions follow both the concerted and stepwise mechanisms. The present work shows that the mechanism actually depends on the substituent. Another interesting finding in the present work is that a small fraction of trajectories of FC(O)N_3 system underwent concerted dissociation but the final isocyanate product isomerized to the nitrene form, pointing to the operation of an indirect mechanism of nitrene production detected in the experiments[Sun *et al.*, 2015; Zeng *et al.*, 2011]. To draw concrete conclusions about the effect of substituents on the mechanism of the Curtius reaction, further studies on more azides are needed.

...

